Viscosity and specific volume of bulk metallic glass-forming alloys and their correlation with glass forming ability

S. Mukherjee [a], J. Schroers [a,b], Z. Zhou [a], W.L. Johnson [a], W.-K. Rhim [a,*]

[a] *Department of Materials Science, Division of Engineering and Applied Science, California Institute of Technology, Mail Code 138-78, Pasadena, CA 91125, USA*
[b] *Liquidmetal Technologies, Lake Forest, CA 92360, USA*

Abstract

The trends in glass formation among bulk metallic glass-forming alloys are investigated within the framework of viscosity and specific volume measurements. This investigation was carried out using four alloys ($Zr_{41.2}Ti_{13.8}Cu_{12.5}Ni_{10}Be_{22.5}$, $Zr_{57}Cu_{15.4}Ni_{12.6}Al_{10}Nb_5$, $Zr_{52.5}Cu_{17.9}Ni_{14.6}Al_{10}Ti_5$ and $Ni_{59.5}Nb_{40.5}$) that have widely different glass forming abilities (GFAs). This study shows that the viscosity at the melting temperature is correlated with volume change upon crystallization in accordance with Cohen–Grest free-volume theory. The viscosity of the best glass former ($Zr_{41.2}Ti_{13.8}Cu_{12.5}Ni_{10}Be_{22.5}$) is found to be an order of magnitude larger compared to the worst glass former ($Ni_{59.5}Nb_{40.5}$) at their respective liquidus temperatures. The other two alloys have intermediate values. The specific volume results also support the trend in GFA with the best glass former showing the smallest volume change upon crystallization and worst glass former showing the largest change. This study suggests that high viscosity and correspondingly small free volume of the liquid at the melting temperature contribute significantly to improve the GFA.
© 2004 Acta Materialia Inc. Published by Elsevier Ltd. All rights reserved.

Keywords: Metallic glasses; Bulk amorphous materials; Kinetics; Undercooling; Glass forming ability

1. Introduction

From the early days of the discovery of metallic glasses it was noticed that liquid viscosity plays a crucial role in the glass forming ability (GFA) of an alloy [1]. High temperature viscosity governs the crystallization kinetics close to the melting point and hence the critical cooling rate for vitrification [2]. Also, the knowledge of high temperature viscosity has engineering importance in casting processes and composite infiltration. Although viscosity data close to the glass transition region exist for quite a few bulk metallic glasses (BMG), only limited amount of data are available for the high temperature region. Viscosity data around the melting temperature of a BMG are much more difficult to obtain

because the reaction of BMG melts with container walls at elevated temperatures give erroneous viscosity values. Sophisticated custom-made equipment [2,3] as well as levitation experiments [4,5] were used to explore the viscosity in the region around the melting temperature. Because of limited viscosity data close to melting point, no systematic study involving high-temperature viscosity has been reported for alloys with different GFA.

The Cohen–Grest model [6] suggests a correlation of free volume with viscosity. The free volume of a liquid reflects the packing density and hence mobility of atoms. A liquid with densely packed atoms will show larger viscosity and a smaller change in volume upon crystallization. Indeed, the volume change upon crystallization for a number of exceptionally good glass formers is significantly smaller than the volume change in pure metals [7–9].Thus it is expected that correlations between viscosity and volume changes of the liquid will have profound ramifications for understanding of the glass formation process.

* Corresponding author. Tel.: +1-626-395-8607; fax: +1-626-795-6132.

E-mail address: won-kyu.rhim@caltech.edu (W.-K. Rhim).

In this paper, we report the viscosities and specific volumes measured over a large temperature range for four BMGs with widely different GFAs, $Zr_{41.2}Ti_{13.8}Cu_{12.5}$ $Ni_{10}Be_{22.5}$ (Vit1), $Zr_{57}Cu_{15.4}Ni_{12.6}Al_{10}Nb_5$ (Vit106), $Zr_{52.5}Cu_{17.9}Ni_{14.6}Al_{10}Ti_5$ (Vit105), and $Ni_{59.5}Nb_{40.5}$ eutectic alloy (NiNb). The measured thermophysical properties are correlated with the GFAs of these alloys. The specific volumes and high temperature viscosities of these alloys are measured using a high vacuum electrostatic levitator (ESL) to avoid heterogeneous influences of containers.

2. Experimental procedure

The alloys were prepared from high purity starting materials in an arc melter. The glass transition temperatures (T_g) and the liquidus temperatures (T_L) were obtained in a differential scanning calorimeter (DSC) and differential thermal analyzer (DTA), respectively, for Vit1, Vit106 and Vit105 at a heating rate of 0.33 K s^{-1}. For the $Ni_{59.5}Nb_{40.5}$ eutectic alloy, the T_g could not be measured directly. It was estimated to be 920 ± 20 K from earlier publications [10,11]. The T_g and T_L values for all the four alloys investigated in this study are listed in Table 1.

Small samples (~15 mg) were levitated in the ESL and melted using a high power continuous wave Nd-YAG laser operating at 1.064 μm. The temperature was measured remotely using a two-color pyrometer with a nominal sensitivity range of 650–1650 K. The cooling curve of each sample was measured by shutting off the laser completely, allowing the sample to cool in a purely radiative way. For the specific volume measurement, the sample images were captured by a CCD camera with a telescopic head and the sample volumes were extracted from it by Legendre polynomial fitting. A detailed description of the density measurement technique is given elsewhere [12]. For the viscosity measurements, the resonant oscillation of the molten drop was induced by an alternating current (AC) electric field while holding the sample at a preset temperature. Viscosity was calculated from the decay time constant of free oscillation that followed the excitation pulse [13]. A detailed description of the ESL facility itself is given in an earlier publication [14]. For Vit106, the viscosity close to the glass transition temperature was determined from measured flow

stresses. Samples of dimension 3 mm × 3 mm × 6 mm were compressed with a quasi-static strain rate of $\gamma = 10^{-4}$ s^{-1} in an MTS 810 machine with a 22,000 lbs MTS 661.20F-03 load cell. The experiments were carried out isothermally and the temperatures were measured with K-type thermocouples. The equilibrium viscosity (η) was determined by $\eta = \sigma_f/\gamma$, where σ_f denotes the experimentally determined equilibrium flow stress. However, this method could not be used to measure the viscosities of Vit105 and NiNb close to T_g because of their size limitations and relatively poor thermal stability against crystallization.

3. Results

Typical free radiative cooling curves obtained for the four alloys are shown in Fig. 1. A pronounced overheating effect was observed for all the alloys. Maximum undercooling was achieved only after the samples were heated above a critical temperature [15]. Vit1 and Vit106 could be fully vitrified by free cooling in the ESL while Vit105 and $Ni_{59.5}Nb_{40.5}$ eutectic alloy crystallized after a certain degree of undercooling. The maximum undercooling achieved for Vit105 was 230 K and that for the $Ni_{59.5}Nb_{40.5}$ eutectic alloy was 130 K. The maximum undercooling as a percentage of the liquidus temperature $(\Delta T/T_L)$ and the critical cooling rates to vitrify the
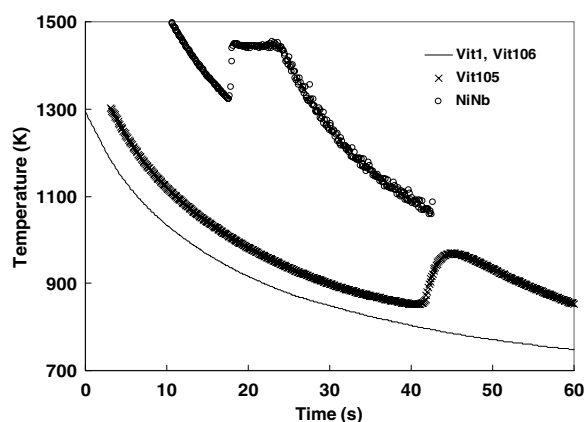

Fig. 1. Free radiative cooling curves for Vit1, Vit106, Vit105, and NiNb. Vit1 and Vit106 could be vitrified by free radiative cooling in the ESL. However, Vit105 and NiNb crystallized after certain undercooling.

Table 1
Characteristic temperatures and critical cooling rates

BMG	T_g (K)	T_L (K)	T_g/T_L	$\Delta T/T_L$ (%)	Critical cooling rate (K s^{-1})
Vit1	620	993	0.624	Vitrified	2
Vit106	682	1115	0.612	Vitrified	10
Vit105	675	1090	0.619	21	25
NiNb	920	1448	0.635	9	250

samples are shown in Table 1. The critical cooling rates vary over two orders of magnitude for the four alloys indicating their widely different GFAs, Vit1 being the best and NiNb being the worst glass formers. The critical cooling rates for Vit1 and Vit106 were measured from their respective time–temperature–transformation (TTT) curves [15], while those of Vit105 and NiNb were estimated from critical casting thickness to form fully amorphous plates [11,16].

The dynamic viscosities as a function of temperature for Vit1 and NiNb alloy measured using the drop oscillation technique are shown in Fig. 2. For Vit1, viscosity could be measured from 1280 K down to 1120 K which was about 130 K above the liquidus temperature. The viscosity increased from 25 mPa s at the high temperature end to an average value of about 160 mPa s at 1120 K. Noise level of the measured viscosity became larger with lowering of temperature because of the increased resistance to oscillation. The average error in viscosity measurement from the decay times at the low temperature end was estimated to be within ±5%. Viscosity of Vit1 close to T_g was measured earlier by Waniuk et al. [17] using three-point beam bending technique. For $Ni_{59.5}Nb_{40.5}$, measurements were carried between 1690 and 1390 K and the viscosity increases from 10 to 80 mPa s. The relatively low viscosity of the NiNb alloy made viscosity measurement possible down to about 60 K undercooling. For Vit106 and Vit105, high temperature viscosities were obtained using the drop oscillation technique in the temperature range from 1360 K to their liquidus temperatures. The range of viscosity is almost same as Vit1 (25–180 mPa s) and hence are not indicated in Fig. 2. For Vit106, low temperature viscosity was determined from measured flow stresses. The viscosity increases from a value of 2×10^{11} mPa s at a temperature 36 K above T_g to a value of about 10^{15} mPa s at T_g.

The measured specific volume for Vit105 as a function of time is shown in Fig. 3. The corresponding cooling curve is also indicated in the figure. On the temperature–time curve, crystallization is evidenced by recalescence, the sharp rise in temperature due to the release of the latent heat of fusion. However, at this large undercooling, the heat released during recalescence was not sufficient to raise the sample to the melting temperature. On the volume–time curve, crystallization is evidenced by the discontinuous decreases in the sample volume. The noise level in the volume data for the crystal is about twice that of the liquid due to slight deformation of the sample upon crystallization. The liquid and crystal specific volumes were extracted separately and plotted as a function of temperature in Fig. 4. The measurement accuracy as shown for Vit105 in Fig. 4 is representative of the results for all other alloys obtained in this study except the crystalline volumes for the NiNb alloy. Severe shape distortion for the NiNb alloy

Fig. 3. Cooling curve and specific volume measured during cooling of Vit105.
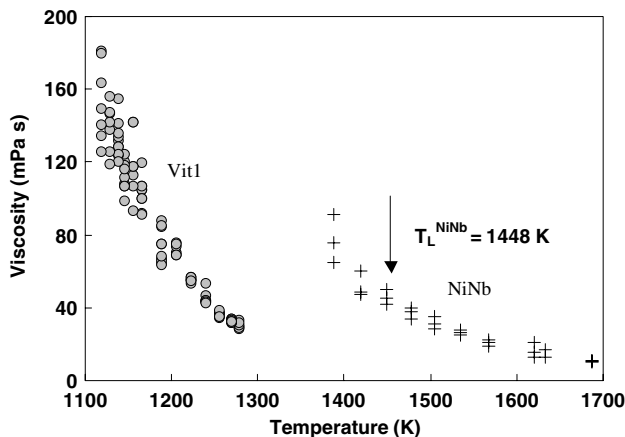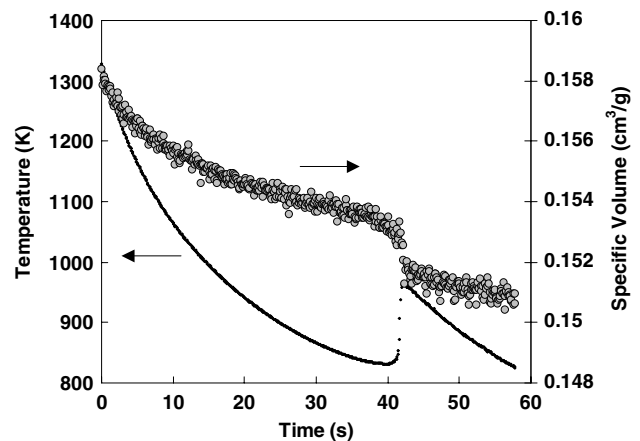

Fig. 2. Viscosity versus temperature for Vit1 and NiNb alloys. The melting temperature for NiNb alloy (1448 K) is indicated. For Vit1, the lowest temperature to which viscosity could be measured by the drop oscillation technique is 130 K above its liquidus temperature.
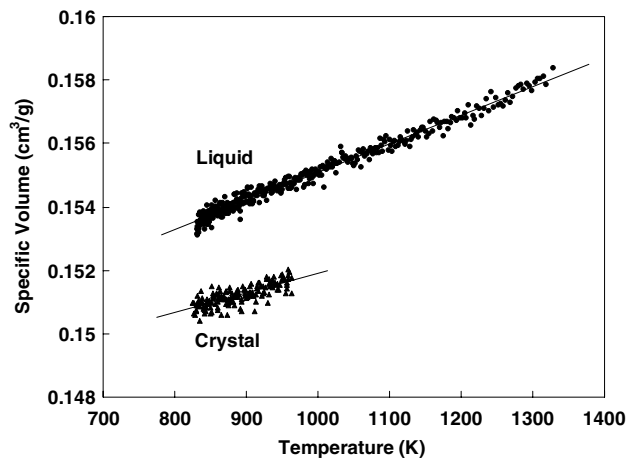

Fig. 4. Liquid and crystalline specific volumes as a function of temperature for Vit105.

Table 2
Specific volume related quantities and volume change upon crystallization

BMG	V_{Liq}^m (cm³ g⁻¹)	α_{Liq} (10⁻⁵ K⁻¹)	V_{Cry}^m (cm³ g⁻¹)	α_{Cry} (10⁻⁵ K⁻¹)	$\Delta V^m / V_{Cry}^m$ (%)
Vit1	0.1668	5.3340	0.165	4.5175	1.09
Vit106	0.1502	5.3291	0.1468	3.2996	2.32
Vit105	0.1559	5.8464	0.1525	4.0602	2.23
NiNb	0.1199	6.8117	0.116	–	3.36

upon crystallization allowed us to obtain only an average value for the crystal specific volume at the melting temperature. The measurement accuracy of liquid specific volume is estimated to be within ±0.1% and of the crystal is about twice of that.

The specific volume $V(t)$ at a temperature T is fit with an equation of the form:

$$V(T) = V^m[1 + \alpha(T - T^m)], \qquad (1)$$

where α is the volume expansion coefficient, T^m is the melting (or liquidus) temperature and V^m is the specific volume at the melting (or liquidus) temperature. The liquid and crystalline specific volumes at the liquidus temperatures (V_{Liq}^m, V_{Cry}^m) and the volume expansion coefficients (α_{Liq}, α_{Cry}) for the four alloys are summarized in Table 2. Our values of the liquid and crystalline specific volumes for Vit1 show good agreement with previous results obtained by Ohsaka et al. [8] using the ESL. The volume change of the liquid upon crystallization was expressed as a percentage of the crystal volume ($\Delta V^m / V_{Cry}^m$) at the liquidus temperature as shown in the last column of Table 2.

4. Discussion

In an earlier work, Turnbull predicted that the T_g/T_L value for good glass formers should be close to 2/3 [1] and it was used as a rule of thumb for predicting the GFA of bulk glass-forming alloys [18]. However, as given in Table 1, the T_g/T_L values for the four alloys investigated in this study are fairly close, being in the range 0.61–0.64, and they do not explain the widely different critical cooling rates for vitrification of these alloys. Also, the thermodynamic driving force for crystallization given by the difference in Gibbs free energies of the liquid and crystal are very similar for Vit1, Vit106 and Vit105 [19], failing to explain their order of magnitude difference in critical cooling rates. So the trends in glass formation are analyzed within the framework of the measured thermophysical properties, viscosity and specific volume, which determine the degree of atomic mobility and hence the crystallization kinetics.

Within Angell's [20] fragility concept, viscosity of liquids has been correlated with their GFA. Use of glass transition temperature (T_g) as the scaling temperature for viscosity allows for classification of liquids according to their "strong-fragile" behavior. Strong liquids show

close to Arrhenius temperature dependence of viscosity and form stable glasses. Fragile liquids, on the other hand, show low viscosity at the melting temperature only to rise sharply close to the glass transition and form glasses which are unstable with respect to crystallization. The fragility behavior shows a correlation with GFA for BMGs with all metallic constituents [17,21]. However, the behavior of metal-metalloid BMGs such as Pd–Ni–Cu–P do not follow the same trend [22]. The difference in fragility behavior for these two classes of alloys has been attributed to the difference in their liquid structure [23].

Fig. 5 is the fragility plot for the alloys investigated in this study. Also shown in the figure are the viscosities of silica (SiO₂) [20], which is a canonical example of a strong glass, showing Arrhenius temperature dependence of viscosity. The viscosity values for Vit105 are identical to Vit106 within experimental scatter. Also shown in Fig. 5 are the viscosities of Vit1 close to T_g that were measured by Waniuk et al. [17] using the three-point beam bending method and the high temperature viscosities that were measured by Masuhr et al. [2] using a Couette viscometer.

As seen from the fragility plot (Fig. 5) and also from previous investigations [20–22], the viscosity of most liquids, both metallic and non-metallic, approaches 10¹⁵
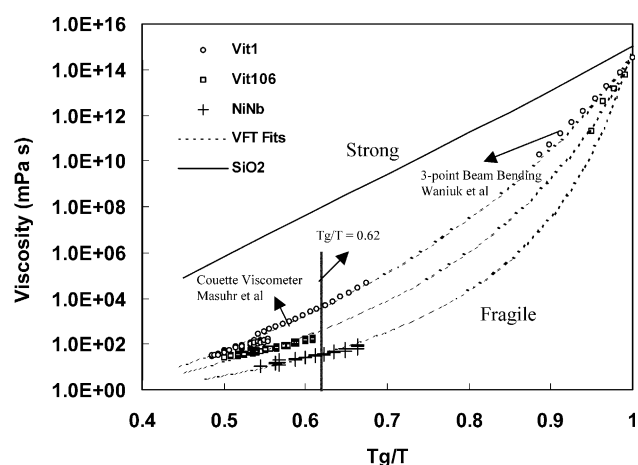

Fig. 5. Fragility plot of viscosity for Vit1, Vit106 and NiNb. Viscosity data for SiO₂ is taken from Angell [20]. Viscosity data for Vit1 measured by Waniuk et al. [17] and Masuhr et al. [2] are indicated by arrows. All the remaining data points are measured in this study. The liquidus temperature for the three alloys is indicated by the vertical line at $T_g/T = 0.62$. The best fits to the experimental data by VFT relations (Eq. (2)) are indicated by the dotted lines.

Table 3
Temperature range for viscosity measurement, melting-temperature viscosities (η_m) and Vogel–Fulcher–Tammann (VFT) fitting parameters (Eq. (2))

BMG	Temperature range (K)	η_m (mPa s)	η_o (mPa s)	D	T_o (K)
Vit1	1118–1278	4835	0.001	23.8	390.0
Vit106	678–718; 1120–1360	200	0.015	11.3	524.7
Vit105	1095–1360	180	0.01	11.6	521.0
NiNb	1390–1690	45	0.06	5.6	800.0

mPa s at the calorimetric glass transition temperature. This is the value assumed for the viscosity of Vit105 and NiNb at their glass transition temperatures. The viscosities measured in this study were fitted (as shown in Fig. 5) with the Vogel–Fulcher–Tammann (VFT) equation [20–22]

$$\eta = \eta_o \exp\left(\frac{DT_o}{T - T_o}\right), \tag{2}$$

where T_o is referred to as the VFT temperature, D is called the "fragility parameter" and η_o is the high temperature limit of viscosity. The three parameters are summarized in Table 3 for all the alloys. A stronger liquid has a higher value of the fragility parameter. The best glass former (Vit1) has the highest $D (= 23.8)$, while the worst glass former (NiNb) is found to be most fragile ($D = 5.6$). So Vit1 is a much stronger liquid compared to the NiNb eutectic alloy and this strong liquid behavior contributes towards better GFA of Vit1. The fragility parameters for Vit105 and Vit106 are very close to each other ($D \sim 11.5$) showing their similar GFA. Thus, for the four bulk metallic glasses investigated in this study, GFA is better for the stronger liquid.

The ratio of glass transition temperature to the liquidus temperature for the alloys investigated in this study is close to 0.62. The liquidus temperature is indicated by a line at $T_g/T = 0.62$ in Fig. 5. The best glass former (Vit1) has about two orders of magnitude higher viscosity compared to the worst glass former (NiNb) at their respective liquidus temperatures. The viscosities of Vit106 and Vit105 lie in-between the two. The range of temperature over which viscosity was measured and the viscosity values at the liquidus temperature (η_m) are shown in Table 3. Clearly, the glass forming ability of the four BMGs scales with their melting-temperature viscosity, η_m. Also, the stronger liquid is found to have higher viscosity at its melting temperature compared to a fragile liquid. Thus, the melting-temperature viscosity follows the same trend as the fragility parameter.

Viscosity can be correlated with the free volume of the liquid using the Cohen–Grest model as [6]

$$\eta = \eta_o \exp\left(bv_m/v_f\right), \tag{3}$$

where v_f denotes the average free volume per atom and bv_m the critical volume for flow. According to Eq. (3), larger viscosity corresponds to smaller free volume which in turn corresponds to denser packing of atoms in

the liquid state. So a high viscosity liquid will show a smaller change in volume upon crystallization. The specific volume data in Table 2 support this argument showing that the best glass former (Vit1) with high melting-temperature viscosity has the smallest change in volume (1.09%) upon crystallization while the worst glass former ($Ni_{59.5}Nb_{40.5}$) has the largest volume change (3.36%). Recently, Shen et al. [24] reported a similar trend during crystallization of the amorphous samples upon heating in the supercooled liquid region. They found that alloys having smallest density difference between amorphous and crystalline states revealed the largest supercooled liquid region [24] and larger supercooled liquid region correlates with better GFA [25]. This implies that denser the packing of atoms in the glass compared to the corresponding crystal, better is the GFA, which is in fact the trend we observe in this study.

Fig. 6 shows the viscosity and volume change upon crystallization at liquidus temperature versus the critical cooling rate for the BMGs investigated in this study. It is clear that smaller critical cooling rate is observed for alloys with higher melting-temperature viscosity which translates to a smaller volume change upon crystallization. This suggests that high temperature viscosity and
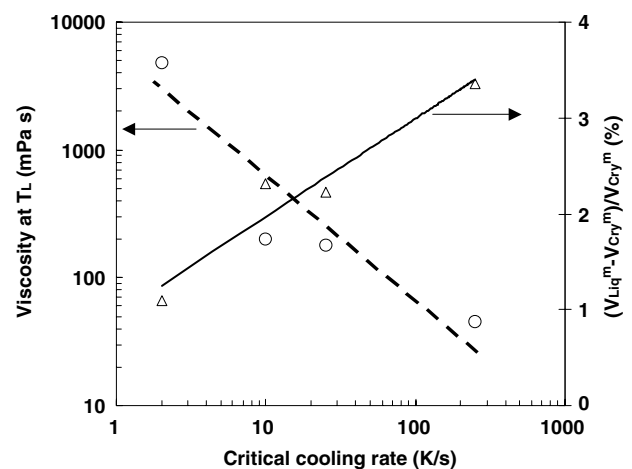

Fig. 6. Viscosity at liquidus temperature (○) and volume change upon crystallization (△) versus critical cooling rate. The solid line shows the trend for volume change upon crystallization and the dotted line shows the trend for viscosity.
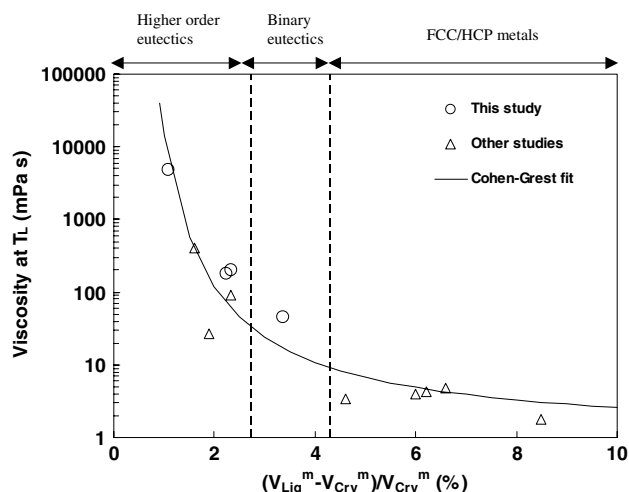
Fig. 7. Viscosity at liquidus temperature versus the volume change upon crystallization for several eutectic alloys and pure metals. In order of increasing volume change the data points are for: Vit1 (present work), $Pd_{43}Ni_{27}Cu_{10}P_{20}$ [9,22], $Pd_{40}Ni_{40}P_{20}$ [3,7], Vit105 (present work), Vit106 (present work), $Zr_{55}Al_{20}Co_{25}$ [28], NiNb (present work), and pure metals (Ti, Zr, Cu, Ni, Al [26,27]). Cohen–Grest free volume fit [6] is indicated.

free volume, which govern the crystallization kinetics close to the melting temperature, have a pronounced influence on the critical cooling rate for vitrification.

Fig. 7 shows the viscosity versus the volume change upon crystallization for several eutectic alloys (or close to eutectic compositions) and pure metals at the melting temperature, including the alloys investigated in this study. The constituent elements (Ti, Zr, Cu, Ni, Al), which have face-centered cubic (FCC) and hexagonal close-packed (HCP) crystal structures, show large volume change upon crystallization [26,27] compared to the higher order eutectic alloys investigated in this study or reported elsewhere [7,9]. Also, the viscosities of pure metals [26] are orders of magnitude lower compared to the higher order alloys [3,22,28]. As shown in Fig. 7, all the data points can be reasonably fitted with the equation: $\eta_m = 0.98 \times \exp[9.76 \times V_{Cry}^m/\Delta V^m]$ mPa s, which is of the same form as Eq. (3) with v_f/v_m being proportional to $\Delta V^m/V_{Cry}^m$. Thus, the melting-temperature viscosity is correlated with excess volume in the liquid for a wide variety of alloys. These results are consistent with the Cohen–Grest free volume theory [6] because a smaller change in volume upon crystallization implies little free volume in the liquid and correspondingly lower atomic mobility which leads to higher viscosity.

5. Conclusions

Viscosity and specific volumes (liquid and crystalline) were measured over a wide temperature range for four alloys with widely different GFAs. The better glass former has higher viscosity at its liquidus temperature and shows a correspondingly smaller change in volume upon crystallization compared to a poorer glass former. The viscosity at the melting temperature is correlated with volume change upon crystallization in accordance with Cohen–Grest free-volume theory. The high-temperature viscosity and the free volume of the liquid have a pronounced influence on the critical cooling rate for vitrification and their knowledge is imperative in understanding the crystallization kinetics of bulk metallic glasses.

References

[1] Turnbull D. Contemp Phys 1969;10:473.
[2] Masuhr A, Waniuk TA, Busch R, Johnson WL. Phys Rev Lett 1999;82:2290.
[3] Tsang KH, Lee SK, Kui HW. J Appl Phys 1991;70:4837.
[4] Egry I, Lohofer G, Seyhan I, Schneider S, Feuerbacher B. Appl Phys Lett 1998;73:462.
[5] Egry I, Lohofer G, Seyhan I, Schneider S, Feuerbacher B. Int J Thermophys 1999;20:1005.
[6] Cohen MH, Grest GS. Phys Rev B 1979;20:1077.
[7] Chow KC, Wong S, Kui HW. J Appl Phys 1993;74:5410.
[8] Ohsaka K, Chung SK, Rhim W-K, Peker A, Scruggs D, Johnson WL. Appl Phys Lett 1997;70:726.
[9] Lu IR, Gorler GP, Willnecker R. Appl Phys Lett 2002;80:4534.
[10] Choi-Yim H, Xu D, Johnson WL. Appl Phys Lett 2003;82:1030.
[11] Leonhardt M, Loser W, Lindenkreuz HG. Acta Mater 1999;47:2961.
[12] Chung SK, Thiessen DB, Rhim W-K. Rev Sci Instrum 1996;67:3175.
[13] Rhim W-K, Ohsaka K, Paradis PF, Spjut RE. Rev Sci Instrum 1999;70:2796.
[14] Rhim W-K, Chung SK, Barber D, Man KF, Gutt G, Rulison A, et al. Rev Sci Instrum 1993;64:2961.
[15] Mukherjee S, Zhou Z, Schroers J, Johnson WL, Rhim W-K. Appl Phys Lett 2004 [in press].
[16] Lin XH, Johnson WL. J Appl Phys 1995;78:6514.
[17] Waniuk TA, Busch R, Masuhr A, Johnson WL. Acta Mater 1998;46:5229.
[18] Johnson WL. MRS Bull 1999;10:42.
[19] Glade SC, Busch R, Lee DS, Johnson WL, Wunderlich RK, Fecht H-J. J Appl Phys 2000;87:7242.
[20] Angell CA. Science 1995;267:1924.
[21] Busch R, Bakke E, Johnson WL. Acta Mater 1998;46:4725.
[22] Fan GJ, Fecht H-J, Lavernia EJ. Appl Phys Lett 2004;84:487.
[23] Fan GJ, Wunderlich RK, Fecht H-J. Mat Res Soc Symp Proc 2003;754:CC5.9.1.

[24] Shen TD, Harms U, Schwarz RB. Appl Phys Lett 2003;83:4512.
[25] Shen TD, Schwarz RB. Appl Phys Lett 1999;75:49.
[26] Iida T, Guthrie RIL. The physical properties of liquid metals. Oxford: Clarendon; 1988.
[27] Buch A. Pure metals properties. Materials Park (OH): ASM International; 1999.
[28] Mukherjee S, Kang H-G, Johnson WL, Rhim W-K. Phys Rev B 2004 [in review].